High Resolution Prediction of Gas Injection Process Performance for Heterogeneous Reservoirs

Quarterly Report
October 1, 2003 to December 31, 2003

Contract No. DE-FC26-00BC15319

Principal Investigator: Franklin M. Orr, Jr.
Department of Petroleum Engineering
Stanford University

Disclaimer

This report was prepared as an account of work sponsored by an agency of the United States Government. Neither the United States Government nor any agency thereof, nor any of their employees, makes any warranty, express or implied, or assumes any legal liability or responsibility for the accuracy, completeness, or usefulness of any information, apparatus, product, or process disclosed, or represents that its use would not infringe privately owned rights. Reference herein to any specific commercial product, process, or service by trade name, trademark, manufacturer, or otherwise does not necessarily constitute or imply its endorsement, recommendation, or favoring by the United States Government or any agency thereof. The views and opinions of authors expressed herein do not necessarily state or reflect those of the United States Government or any agency thereof.

Abstract

In this report we present an approach for accurate and consistent implementation of gravity effects in compositional streamline simulation.

The approach is based on an operator-splitting technique, successfully applied in streamline simulation of black-oil models. The method is demonstrated to conserve mass. Its application adds only marginally to the overall CPU requirement. We provide a detailed description of the approach to incorporate gravity effects and demonstrate the efficiency of compositional streamline simulation, even for cases where gravity segregation plays an important role in the overall process performance.

The new approach is demonstrated to be in excellent agreement with commercial FD simulators for prediction of flows in 2D vertical and multi-well 3D geometries. Finally, we outline the work required to extend the compositional streamline approach to handle three-phase flow modeling, also including gravity.

Table of Contents

Executive Summary 1
1. Introduction 2
2. Experimental 2
3. Mathematical Formulation 3
4. Solution along Gravity Lines 5
5. Calculation Examples 7
   5.1. 2D Homogeneous displacement 8
   5.2. 2D Heterogeneous displacement 8
   5.3. 3D Quarter five spot 9
   5.4. 3D Five spot 9
6. Results and Discussion 10
7. Conclusions 11
8. Acknowledgment 11
9. Nomenclature 12
10. References 13

Executive Summary

Conventional finite-difference (FD) or finite-element simulators are presently too slow to permit high resolution compositional simulation at field scale. However, the application of compositional streamline simulation has so far been limited to production scenarios where effects of gravity can be neglected. The lack of suitable methods to include gravity effects has restricted the use of compositional streamline simulation to 2D horizontal displacement problems or 3D displacement problems for fluids with a low-density contrast

The aim of this work is to extend the area of applicability for compositional streamline simulation by suggesting an efficient method to include gravity segregation on the list of represented physics that control processes performance of gas injection schemes at field scale.

We start by reviewing the conservation equations for multiphase multicomponent flows in porous media with particular emphasis on handling gravity segregation in compositional streamline simulation. Next, we describe an efficient approach for including the effects of gravity. We then demonstrate, through a series of 2D and 3D example calculations, the accuracy of the suggested approach by comparing simulation results with those of a commercial finite difference based simulator.

For the 2D example calculations, the implementation of the presented approach in our research code, CSLS, requires 12-15 times less CPU time than the equivalent finite difference based IMPES simulation. For the larger calculation examples, CSLS required 20 times less CPU time than the FD IMPES simulation and 2-3 times less CPU time than the equivalent FD AIM simulation.

The presented approach to incoorporate gravity effects in compositional streamline simulation is easily extended to handle three-phase flows (e.g. for simulation of WAG problems), but has not yet been implemented in our research code, CSLS.

1. Introduction

Compositional streamline simulation for assessment of miscible/near-miscible gas injection process performance has significant potential to accommodate requirements for accurate and reliable production forecasts. These requirements include high resolution descriptions of permeability heterogeneity and an appropriate representation of the phase behavior including a sufficient number of components in the equation of state representation of the reservoir fluid. The combination of high spatial resolution and sufficient compositional resolution is needed to resolve the complex coupling between flow and phase behavior.

Conventional finite-difference (FD) or finite-element simulators are presently too slow to permit high resolution compositional simulation at field scale. However, the application of compositional streamline simulation has so far been limited to production scenarios where effects of gravity can be neglected. The lack of suitable methods to include gravity effects has restricted the use of compositional streamline simulation to 2D horizontal displacement problems or 3D displacement problems for fluids with a low-density contrast.

The aim of this work is to extend the area of applicability for compositional streamline simulation by suggesting an efficient method to include gravity segregation on the list of represented physics that control processes performance of gas injection schemes at field scale. Numerous authors have contributed significantly to the development of streamline simulation in general[1-15]. We refer the reader to these contributions for detailed coverage of the fundamentals of streamline simulation.

In the following sections, we start by reviewing the conservation equations for multiphase multicomponent flows in porous media with particular emphasis on handling gravity segregation in compositional streamline simulation. Next, we describe an efficient approach for including the effects of gravity. We then demonstrate, through example calculations, the accuracy of the suggested approach by comparing simulation results with those of a commercial finite difference based simulator.

2. Experimental

This report describes a new approach for implementiung gravity effects in compositional streamline simulation. Hence, no experimental work is reported.

3. Mathematical Formulation

In this section we present the mass conservation equations for multicomponent multiphase flows with emphasis on including gravity segregation in compositional streamline simulation. If effects of dispersion are neglected, mass conservation of n_c components distributed in n_p phases, flowing through a heterogeneous porous medium can be written as[16]

$$\phi\frac{\partial}{\partial t}\left\{\sum_{j=1}^{n_p}\omega_{ij}\rho_{mj}S_j\right\}+\nabla\left\{\sum_{j=1}^{n_p}\omega_{ij}\rho_{mj}\underline{u}_j\right\}=0\,,\quad i=1,..,n_c \tag{1}$$

where ϕ is the porosity, t is the time, ω_{ij} is the mass fraction of component *i* in phase *j*, ρ_{mj} is the mass density of phase *j*, S_j is the gas saturation and u_j is the velocity of phase *j*. According to Darcy's law, the velocity of phase *j* can be written in terms of the total permeability (k), the relative permeability of phase *j* (k_{rj}), the viscosity (μ_j) and the mass density (ρ_{mj}) of phase *j*

$$\underline{u}_j=-\frac{\underline{\underline{k}}k_{rj}}{\mu_j}\left(\nabla p+\rho_{mj}g\nabla D\right),\ j=1,..,n_p \quad , \tag{2}$$

where p, D and g are the pressure, depth and gravity (capillary effects are not included). For flow problems that are strongly coupled to the phase behavior of the flowing phases, it is more convenient to work with the conservation equations stated in terms of mole fractions and molar densities;

$$\phi\frac{\partial}{\partial t}\{C_i\}+\nabla\left\{\sum_{j=1}^{n_p}x_{ij}\rho_j\underline{u}_j\right\}=0\,,\quad i=1,..,n_c \quad , \tag{3}$$

with

$$C_i=\sum_{j=1}^{n_p}x_{ij}\rho_jS_j\,,\quad i=1,..,n_c \quad , \tag{4}$$

where x_{ij} is the mole fraction of component *i* in phase *j* and ρ_j is the molar density of phase *j*. For convenience we introduce the overall molar flux F_i

$$F_i=\underline{u}_t\sum_{i=1}^{n_p}x_{ij}\rho_jf_j\,,\ i=1,..,n_c \quad , \tag{5}$$

where f_j is the fractional flow of phase j and rewrite Eq. (3) as

$$\phi\frac{\partial}{\partial t}\{C_i\}+\nabla\{F_i\}=0\,,\quad i=1,..,n_c \quad . \tag{6}$$

In compositional streamline simulation, Eq. (6) is decomposed into a sequence of 1D displacement problems along streamlines[11,13,15]. As streamlines are trajectories in space, dictated by the total velocity field, propagation of fluids along the streamlines does not account for gravity effects driven by differences in density between the flowing phases unless explicitly included in terms of in the fractional flow function f_j. Lake[16] demonstrates how gravity can be included in the fractional flow function for immiscible flows. However, including gravity in the fractional flow function allows for negative wave velocities and hence complicates the use of

otherwise efficient upwind schemes. Another possibility is to locate phase specific streamlines as discussed by Blunt et al.[7]

Operator splitting is an alternative for including gravity in streamline based simulation and has been applied successfully for immiscible flows by several investigators[6,8,10]. To include gravity by operator splitting, the flux term in Eq. (6) must be expanded into a convective term accounting for gradients in pressure and a gravity term accounting for gradients in mass density.

In the following derivation we assume that the gravity vector is aligned with the z axis in Cartesian coordinates. By summing Eq. (2) over all phases, the vertical portion of the total velocity (u_z) can be written as

$$u_z = -k_z\left(\lambda_t \frac{\partial p}{\partial z} + \lambda_g \frac{\partial D}{\partial z}\right) = \sum_{j=1}^{n_p} u_{z,j} \quad , \tag{7}$$

with the total mobility (λ_t) and the total gravity mobility (λ_g) given by

$$\lambda_t = \sum_{j=1}^{n_p} \lambda_j = \sum_{j=1}^{n_p} \frac{k_{rj}}{\mu_j} \qquad \lambda_g = g\sum_{j=1}^{n_p} \lambda_j \rho_{mj} \quad . \tag{8}$$

By substituting the Darcy velocity into Eq. (3), the conservation equations can be rewritten along a gravity line (vertical line) as

$$\phi \frac{\partial}{\partial t}\{C_i\} - \frac{\partial}{\partial z}\left\{\sum_{j=1}^{n_p} x_{ij}\rho_j K_z \lambda_j \left(\frac{\partial p}{\partial z} + \rho_{mj} g \frac{\partial D}{\partial z}\right)\right\} = 0 \quad . \tag{9}$$

To eliminate the pressure gradient from Eq. (9), Eq. (7) is rewritten as

$$\frac{\partial p}{\partial z} = -\frac{u_z}{k_z \lambda_t} - \frac{\lambda_g}{\lambda_t}\frac{\partial D}{\partial z} \quad , \tag{10}$$

and finally by inserting Eq. (10) into Eq. (9) we obtain

$$\phi \frac{\partial}{\partial t}\{C_i\} + \frac{\partial}{\partial z}\{F_i^*\} + \frac{\partial}{\partial z}\{G_i\} = 0 \,, \quad i = 1,..,n_c \quad , \tag{11}$$

where F_i^* is the vertical convective flux of component i given by

$$F_i^* = u_z \sum_{j=1}^{n_p} x_{ij}\rho_j f_j \,, \quad i = 1,..,n_c \quad , \tag{12}$$

and G_i is the gravity driven flux of component i given by

$$G_i = k_z \sum_{j=1}^{n_p} x_{ij}\rho_j \lambda_j \left(\frac{\lambda_g}{\lambda_t} - \rho_{mj} g\right)\frac{\partial D}{\partial z} \,, \quad i = 1,..,n_c \quad . \tag{13}$$

In streamline simulation of immiscible flows, the equivalent of Eq. (9) is commonly solved in a sequential manner by operator splitting[6,8,10]. Operator splitting relies on the consistency of treating the convective flux independently from the gravity flux within a given time step of the simulation. In other words, any given time step starts with a convective step solving Eq. (6) along a set of streamlines using the standard Buckley-Leverett form of the fractional flow function

$$f_j = \frac{\lambda_j}{\lambda_t} \quad , \tag{15}$$

followed by a gravity step solving

$$\phi \frac{\partial}{\partial t}\{C_i\} + \frac{\partial}{\partial z}\{G_i\} = 0 \, , \quad i = 1,..,n_c \quad . \tag{16}$$

For small time steps the operator-splitting approximation is fairly accurate whereas large time steps may lead to significant operator-splitting errors. In the following section we discuss the consequences of solving the gravity equation (Eq. 16) including compositional effects.

4. Solution along Gravity Lines

A complication that must be addressed in the use of an operator-splitting technique to account for gravity segregation in compositional flows arises from the fact that the performance of compositional displacements can depend strongly on the displacement path. Consider, for example, a gas front in a two-phase gas/oil displacement invading a sequence of gridlocks along the path a shown in Fig. 1. The corresponding path predicted by an operator-splitting approach could be: A convective step b followed by a gravity step c also shown in Fig. 1. If the gas has a low solubility in the oil phase, the two paths would result in a very similar final states corresponding to a small operator-splitting error. If on the other hand the gas is highly soluble in the oil phase (e.g. in undersaturated reservoir fluids), significant amounts of the gas phase would dissolve in the liquid phase as it moves towards the final state. In the worst case, only a small fraction of the original gas phase remains as the gravity step progresses, resulting in a larger operator-splitting error. Furthermore, liquid contacted by the injected phase will have a different density than the original reservoir fluid and hence lighter liquid may seek upwards. Simultaneous liquid-liquid and vapor-liquid segregation corresponds in principle to a three-phase (water-oil-gas) immiscible system.

To reduce the path dependence as well as the CPU requirement for gravity steps in compositional streamline simulation, we propose a pseudo-immiscible approach illustrated in Fig. 2. At the end of a given convective step, gravity lines are traced. For a Cartesian grid the gravity lines simply correspond to a column of gridblocks. For each gravity line the following steps are performed: equilibrate gridblocks (flash) and record phase saturations, molar densities, viscosities and phase compositions for each gridblock. Each individual phase in a gridblock defines a segment of known composition, molar density, and fluid properties. For two-phase flows, the maximum number of segments along a gravity line is two times the number of gridblocks. This initial state is illustrated in Fig. 2a with gas segments g_1, g_2 and liquid segments l_1 and l_2. The pseudo-immiscible gravity step is then performed by moving segments according to the density contrast and relative permeabilities corresponding to the overall phase saturations. For a given gridblock k, the gas saturation S_k is evaluated summing the saturations of all gas segments present in the gridblock

$$S_k = \sum_{i=1}^{n_s} S_{i,k}^{g} \quad , \tag{17}$$

where $S^g_{i,k}$ is the saturation of gas segment i in gridblock k. Eq. (17) allows the calculation of the relative permeabilities of gas and liquid in any gridblock at any time during a gravity step. Phase viscosities and densities are calculated as saturation averages of the segments present in a gridblock:

$$\mu^g_k = \frac{1}{S_k}\sum_{i=1}^{n_s}\mu^g_{i,k}S^g_{i,k} \tag{18}$$

$$\mu^l_k = \frac{1}{1-S_k}\sum_{i=1}^{n_s}\mu^l_{i,k}S^l_{i,k} \tag{19}$$

$$\rho^g_{m,k} = \frac{1}{S_k}\sum_{i=1}^{n_s}\rho^g_{m,i,k}S^g_{i,k} \tag{20}$$

$$\rho^l_{m,k} = \frac{1}{1-S_k}\sum_{i=1}^{n_s}\rho^l_{m,i,k}S^l_{i,k} \tag{21}$$

Once the phase saturations, relative permeabilities, densities and viscosities are calculated, the saturation of individual segments *i* can be updated from time step n to n+1 by a modified version of the approach for immiscible fluids outlined by Batycky[10]

$$S^{n+1}_{i,k} = S^n_{i,k} - \frac{\Delta t}{\phi \Delta z_k}\left(\tilde{H}_{i,k+1/2} - \tilde{H}_{i,k-1/2}\right) \tag{22}$$

The flux of segment *i* due to gas-liquid segregation is calculated by

$$H_{i,k+1/2} = g\frac{k_{z,k+1}k_{rg,k+1}k_{z,k}k_{ro,k}(\rho_{m,o}-\rho_{m,g})}{\mu_o k_{z,k+1}k_{rg,k+1} + \mu_g k_{z,k}k_{ro,k}} \quad , \tag{23}$$

and

$$\tilde{H}_{i,k+1/2} = H_{i,k+1/2}\sum_{j}^{gas} S_{j,k+1} \tag{24}$$

for gas segments, and

$$\tilde{H}_{i,k+1/2} = -H_{i,k+1/2}\sum_{j}^{liq} S_{j,k} \tag{25}$$

for liquid segments. Similar expressions for liquid-liquid segregation can be derived but need not be repeated. The time step Δt in Eq. (22) is selected by the CFL condition

$$\Delta t = CFL/\max\left(\frac{H_{i,k+1/2}}{\phi}\right) \tag{26}$$

At the end of a gravity step, demonstrated in Fig. 1b, the gas and liquid segments in each gridblock are combined to form a new overall molar density and overall mole fraction of component i on gridblock k by

$$C_{i,k} = \sum_{j=1}^{N_{seg}} z_{i,j,k}\rho_j S_j \tag{27}$$

$$z_{i,k} = C_{i,k} / \sum_{j=1}^{n_c} C_{j,k} \tag{28}$$

The approach described will always conserve mass as the numerical scheme of Eq. (22) conserves the volume of each segment and each segment contains a fixed number of moles determined from the initial state of the gravity line. Furthermore, the CPU requirement of the pseudo-immiscible gravity step is greatly reduced relative to the fully compositional approach, as the gridblocks associated with a gravity line only are flashed at the very beginning of the segregation step.

In the following section we compare the proposed approach with results of simulations performed with the commercial finite difference based simulator, E300. The compositional streamline simulator, CSLS, used in the calculation examples is a modified version of the black-oil simulator, 3DSL, initially developed by Batycky[10]. All calculation examples make use of the Peng-Robinson equation of state to predict phase behavior and the Lohrenz-Bray-Clark correlation to predict phase viscosities.

5. Calculation Examples

For all calculation examples, described in the following sub-sections, the reservoir fluid description given in Table 1 was used. The fluid description is a 6 component representation of the compositional analysis given in Table 2. Throughout the calculation examples, the reservoir temperature was kept constant at 387.45 K. At this temperature the saturation pressure of the reservoir fluid is 220.2 atm. Two injection compositions are used: a separator gas given in Table 1, and pure CO_2. The minimum miscibility pressure (MMP) for injection of the separator gas is 324 atm whereas the MMP for injection of pure CO_2 is 247 atm. Simple quadratic Corey type relative permeability functions were used to determine the phase mobilities.

We present the displacement calculations according to their increasing degree of complexity to gradually build confidence in the predictions of CSLS. The examples include:

- 1D displacement to compare the prediction of local displacement efficiencies predicted by CSLS and E300.
- 2D vertical displacement for a homogeneous porous media with $k_z = 0.1\ k_x$.
- 2D vertical displacement in a heterogeneous porous media with $k_z = 0.1\ k_x$.
- 3D quarter five spot displacement in an isotropic heterogeneous porous media.
- 3D five spot pattern in an isotropic heterogeneous porous media.
- 1D displacement calculation

In the first calculation example the reservoir fluid is displaced by the separator gas at an injection pressure below the MMP. The injection pressure is set at 225 atm and hence the displacement process is sub-miscible. The simulations were performed with 100 grid blocks. Fig. 3 reports the

production history for the 1D displacement in terms of the recovery of OOIP and the gas-oil ratio (GOR) as a function of pore volumes injected (PVI). Fig.1 shows excellent agreement between the recovery predictions for the two simulators whereas small differences are found for the calculated gas-oil ratios. The ultimate recovery predicted by both simulators (~80%) is, as expected for a sub-miscible displacement, well below 100%. However, this simple initial test confirms that the local displacement efficiencies predicted by the simulators are in agreement prior to the analysis of more complicated displacement calculations.

5.1. 2D Homogeneous displacement

In the second calculation example we displace the reservoir fluid by the separator gas at a pressure above the MMP. The 1000 gridblock vertical slice, representing the porous media, measures 100x10x1 meters with k_x = 50 mD and k_z = 5 mD and a porosity of 0.3.

The separator gas in injected over the entire left hand side of the vertical slice at a constant rate of 1.5 Rm3/day corresponding to a front velocity of approximately 1 m pr. Day. The producer is completed in 1 gridblock only, at the lower right hand side of the domain and is operated at a bottom-hole pressure of 325 atm. Hence, the pressure anywhere in the domain will remain above the MMP throughout the displacement.

Fig. 4 compares the distribution of the gas phase saturation after 100 and 200 days of injection (0.5 and 1.0 PVI) as predicted by CSLS and E300. Both simulators predict the formation of a gravity tongue as the low density injection gas propagates along the domain. Small differences between the saturation distributions after 100 days are noticed at the front of the displacement. This may be due to the time step selection for pressure-solves/gravity-steps in the streamline method as addressed in the discussion section. Also, small differences are observed in the column of gridblocks containing the production well. The difference can be attributed to the numerical smearing of the displacement front in the FD formulation of the displacement problem used by E300.

In general, we observe a good agreement between the spatial locations of the gas predicted by the two simulation approaches. A comparison of the predicted recovery and producing gas-oil ratios is shown in Fig.5. For this calculation example, the streamline approach predicts a slightly higher ultimate recovery than the FD simulation on the account of a slightly lower GOR after the gas breaks through to the producer.

5.2. 2D Heterogeneous displacement

In the third calculation example, a heterogeneous permeability field, shown in Fig. 6, was used with $k_z = 0.1 \cdot k_z$. The average (k_x) permeability is 90 mD with a variance of 6000. In this example the reservoir fluid was displaced by pure CO_2 at near miscible conditions. As in previous example the injector is completed over the entire left-most column and the producer is completed in the lower right hand corner. CO_2 was injected at a rate of 1.5 Rm^3/day, and the producer was operated at a bottom-hole pressure of 225 atm.

Fig. 7 shows the gas saturation maps after 50 and 100 days (0.25 and 0.5 PVI) as predicted by CSLS and E300. At early times, the injected CO_2 invades the porous media in a more piston like manner than in the homogeneous case, due to a lower density contrast as well as to the redirection of fluids caused by the heterogeneity. The combined effect results in a better sweep of the lower portion of the reservoir. The redirection of the gas phase is more pronounced after 100 days of injection, where gas from the top of the formation flows downwards through a high

permeable zone. Again, we see good agreement between the saturation distributions predicted by CSLS and E300.

The corresponding production history of the two simulations is shown in Fig. 8. After gas breakthrough, the recovery predicted by CSLS is slightly higher than that predicted by E300. For this displacement, the difference in the predicted recovery is due to numerical diffusion in the FD simulation. Numerical diffusion acts to smear the displacement front reducing the local displacement efficiency relative to that predicted by the streamline approach, while at the same time marginally delaying the breakthrough of the injected gas.

5.3. 3D Quarter five spot

Next, CSLS was tested on a 3D quarter five spot pattern with 25000 (50x50x10) gridblocks. The dimensions of each gridblock are 2x2x2m with a porosity of 0.3. The average kx permeability is 90 mD with a variance of 11000. The injector and producer were completed over the entire column of the domain. In this example CO_2 was injected at a rate of 60 Rm^3/day, and the producer was operated at a bottom-hole pressure of 225 atm. Fig. 9 shows the gas saturation in 3 horizontal slices of the domain (layers 1, 5 and 10) predicted by CSLS and E300 after 300 days (0.3 PVI) of injection.

The predicted saturation distributions are found to be in excellent agreement with only minor variations in local displacement efficiency attributed the different level of numerical diffusion in the two simulation approaches. Fig. 10 shows the predicted recovery and producing GOR for the displacement. The agreement of the production history follows that of the saturation distributions and only minor differences are seen for the predicted recovery after 1.5 PVI.

5.4. 3D Five spot

In the final example calculation, the reservoir fluid is displaced by pure CO_2 at near-miscible conditions. The 3D permeability field from previous example is used for a five-spot pattern with an injector located in the middle of the domain and producers located at each corner. All wells are completed over the entire column of the reservoir. CO_2 is injected at 60 Rm^3/day and the production wells are operated at bottom-hole pressures of 225 atm. The gas saturation distribution after 0.1 PVI (100 days) and 0.2 PVI (200 days) are compared for 3 areal slices in Figs. 11 and 12. Fig. 11 is a snapshot of the displacement process just before the gas arrives at one of the producers, whereas the gas front has reached two producers in Fig. 12. Due to the significant segregation of fluids, the lower portion of the formation is hardly contacted by the injected gas when the top layer breaks through to the producer. Consequently, the ultimate recovery of the initial oil will be relatively low, as Fig. 13 shows. Fig. 13 reports the recovery of the original oil in place and as well as the producing GOR. At 1.5 PVI as little as ~50% of the oil is produced. As in the previous calculation examples, only marginal differences in the front locations as well as in the predicted production history are observed.

6. Results and Discussion

A summary of the CPU requirements for the presented calculation examples is given in Table 3 for the streamline approach and for the FD approach using implicit pressure explicit saturation (IMPES) and adaptive implicit (AIM) modes. For the 2D example calculations the implementation of the presented approach in our research code, CSLS, required 12-15 times less CPU time than the equivalent finite difference based IMPES simulation. For the larger calculation examples, CSLS required 20 times less CPU time than the FD IMPES simulation and 2-3 times less CPU time than the equivalent FD AIM simulation. A potential for additional speed-ups are available through adaptive mesh refinement along streamlines[17].

In the previous sections we have presented and tested a new method, based on operator-splitting, for including gravity effects in compositional streamline simulation. In the presented calculation examples the time between successive gravity steps was estimated based on the number of gridblocks invaded in the horizontal direction. If more than 5 additional gravity lines were required for a 2D calculation and more than 50 additional gravity lines were needed in a 3D calculation, the subsequent time step was reduced by a factor 2. If this constraint was not violated the time step was doubled. A more sophisticated framework for selecting the length of time steps between successive pressure updates/gravity steps has been suggested by Ichiro et al[14] but has not yet been implemented and tested in CSLS.

Traditional methods for recording initial conditions along streamline and reassigning compositions on the pressure grid after a convective/gravity step introduce smearing of saturation fronts as well as mass balance errors. If frequent mapping to and from streamlines is required, special care must be taken to reduce these diffusive errors through the use of higher-order accurate mapping as discussed by Mallison et al.[17].

Extension of the presented approach to three-phase flow modeling is straight forward. The presence of a third phase can add a maximum of ng segments to the problem, where ng is the number of gridblocks along a gravity line. Once the average phase properties are calculated, any 3-phase black-oil formulation can be used to segregate the fluids.

7. Conclusions

The analysis and examples reported lead to the following conclusions.

- A new approach for including effects of gravity in compositional streamline simulation is proposed and demonstrated.

- The new approach offers a consistent and efficient method for extending the applicability of compositional streamline simulation to EOR displacements where gravity segregation can play an important role.

- The implementation of the pseudo-immiscible approach introduces a marginal increase in the overall CPU requirement, as flash calculations are required only to generate the initial state along a gravity line.

- The pseudo-immiscible approach is demonstrated to produce performance predictions in excellent agreement with a commercial finite difference based simulator.

- Through a series of calculation examples, the compositional streamline approach has been demonstrated to be up to 22 faster than equivalent IMPES simulations with a finite difference based simulator.

- The presented approach is easily extended to three-phase flow problems without significant increase in CPU requirements.

8. Acknowledgment

The authors acknowledge with gratitude the support of the US Department of Energy through contract number DE-FC26-00BC15319 and the support of the member companies of the SUPRI-C Gas Injection Industrial Affiliates Program.

9. Nomenclature

C_i : overall molar density of component i
$C_{i,k}$: C_i in gridblock k
D : depth
f_j : fractional flow of phase j
F_i^* : velocity scaled total convective flux of component i
g : gravity constant
G_i : gravity driven flux of component i (compositional formulation)
H_i : gravity driven flux of component i (black-oil formulation)
k : absolute permeability
k_{rj} : relative permeability of phase j
k_z : absolute permeability in z-direction
n_c : number of components
n_p : number of phases
p : pressure
S_j : saturation of phase j
$S^g_{i,k}$: saturation of gas segment i in gridblock k
t : time
u_j : velocity of phase j
u_z : total velocity in z direction
w_{ij} : mass fraction of component i in phase j
x_{ij} : molefraction of component i in phase j
z : distance
$z_{i,k}$: molefraction of component i in gridblock k

Greek symbols

ϕ : porosity
λ_t : total mobility
λ_g : total gravity mobility
μ_j : viscosity of phase j
$\mu^{\alpha}_{i,k}$: viscosity of segment i of phase α in gridblock k
ρ_j : molar density of phase j
$\rho^{\alpha}_{i,k}$: molar density of segment i of phase α in gridblock k
ρ_{mj} : mass density of phase j

10.References

1. Bommer, M.P. and Schechter, R.S: "Mathematical Modeling of In-Situ Uranium Leaching", SPEJ (Dec. 1979) 19, 393-400
2. Bradtvedt, F., Bradtvedt, K., Buchholz, C., Holden, L., Holden, H., and Risebro, N.H. "A New Front-Tracking Method for Reservoir Simulation", SPE Reservoir Engineering, Feb. 1992, 107-116.
3. Datta-Gupta, A. and King, M.J: "A Semi-Analytical Approach to Tracer Flow Modeling in Heterogeneous Permeable Media", Advances in Water Resources (1995) 18, p. 9-24.
4. Thiele, M.R., Blunt, M.J., and Orr, F.M., Jr. 1995a: "Modeling Flow in Heterogeneous Media Using Streamtubes – I. Miscible and Immiscible Displacements" In Situ 19 (4), 299-339.
5. Thiele, M.R., Blunt, M.J., and Orr, F.M., Jr. 1995b: "Modeling Flow in Heterogeneous Media Using Streamtubes – II. Compositional Displacements," In Situ 19 (4), 367-391.
6. Bradtvedt, F., Gimse, T. and Tegnander, C.: "Streamline computations for porous media flow including gravity", Transport in Porous Media, 1996, Vol. 25, No. 1, 63-78.
7. Blunt, M.J., Lui, K. and Thiele, M.R: "A Generalized Streamline Method to Predict Reservoir Flow", Petroleum Geoscience (1996) 2, p. 259-269.
8. Batycky, R.P., Blunt M.J. and Thiele, M.R: "A 3D Field Scale Streamline Simulator with gravity and Changing Well Conditions", SPE 36726, ATCE, Denver, CO, 1996.
9. Thiele, M.R., R.P. Batycky, M.J. Blunt and F.M. Orr, Jr. Simulating Flow in Heterogeneous Media Using Streamtubes and Streamlines. SPE Reservoir Engineering, 10(1), 5-12, 1996.
10. Batycky, R.P: "A Three-Dimensional Two Phase Field Scale Streamline Simulator", Ph.D. dissertation, Stanford University, Dept. of Petroleum Engineering. Stanford CA January 1997
11. Thiele, M.R., Batycky, R.P and Blunt, M.J: "A Streamline-Based 3D Field-Scale Compositional Reservoir Simulator", SPE 38889, ATCE, San Antonio, TX, 1997.
12. King, M.J. and A. Datta-Gupta. Streamline Simulation: A Current Perspective. In Situ, 22(1): 91-140, 1998.
13. Crane, M., F. Bratvedt, K. Bratvedt and R. Olufsen. A Fully Compositional Streamline Simulator, SPE 63156 presented at the SPE Annual Technical Conference and Exhibition, Dallas, TX, October 2000.
14. Ichiro, O., A. Datta-Gupta and M.J. King. Time Step Selection During Streamline Simulation via Transverse Flux Correction. SPE 79688 presented at the SPE Reservoir Simulation Symposium, Houston, TX, February 2003.
15. Seto, C.J., K. Jessen and F.M. Orr, Jr. Compositional Streamline Simulation of Field Scale Condensate Vaporization by Gas Injection. SPE 79690 presented at the SPE Reservoir Simulation Symposium, Houston, TX, February 2003.
16. Lake, L.W.: "Enhanced Oil Recovery", Prentice Hall Publishers, New York City (1989), p. 29.
17. Mallison, B.T., M.G. Gerritsen, K. Jessen and F.M. Orr, Jr. High Order Schemes for Two-Phase Multicomponent Flow, SPE 79691 presented at the SPE Reservoir Simulation Symposium, Houston, TX, February 2003.

	P_c (atm	T_c (K)	ω	M_w	Z_c	x_{oil}	y_{sep}
N_2\C_1	44.61	189.5	0.0085	16.16	0.2898	0.4630	0.8027
CO_2	71.95	304.2	0.2280	44.01	0.2706	0.0164	0.0255
C2-C5	39.89	387.6	0.1673	45.57	0.2759	0.2052	0.1582
C6-13	32.58	597.5	0.3861	117.74	0.2567	0.1911	0.0136
C14-24	17.22	698.5	0.8078	248.83	0.2197	0.0811	0
C25-80	11.39	875.0	1.2314	481.52	0.1825	0.0432	0

0					
0.11883	0				
0.00071	0.15	0			
0.000778	0.15	0	0		
0.01	0.15	0	0	0	
0.011	0.15	0	0	0	0

Table 1: Fluid description used in calculation examples (T_{res} = 387.45 K)

Name	Mole fraction	Name	Mole fraction	M_w (g/mole)	ρ (g/cm^3)
N2	0.0045	C7	0.0377	92	0.7294
CO2	0.0164	C8	0.0428	106	0.7509
H2S	0.0000	C9	0.0270	120	0.7739
Methane	0.4585	C10	0.0169	137	0.7835
Ethane	0.0715	C11+	0.1658	288	0.8835
Propane	0.0674				
i-Butane	0.0084				
n-Butane	0.0311				
i-Pentane	0.0103				
n-Pentane	0.0165				
Hexane	0.0252				

Table 2: Compositional description used for reservoir fluid characterization.

Displacement	$N_{gridblock}$	E300 - AIM	E300 - IMPES	CSLS
2D – homogeneous	1000	N.A.	271 sec	22 sec
2D – heterogeneous	1000	N.A.	398 sec	26 sec
3D – quarter five spot	25000	7457 sec	59353 sec	2701 sec
3D – 5-spot	25000	3356 sec	36568 sec	1680 sec

Table 3: Summary of CPU requirements in seconds (2.8 GHz)

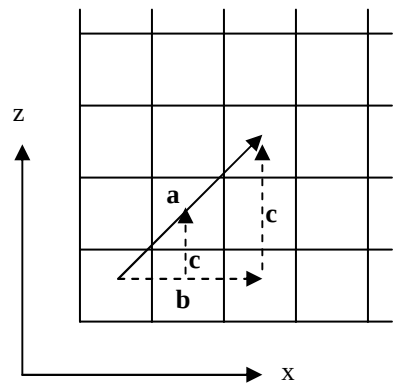

Figure 1: Path dependence of compositional flows.

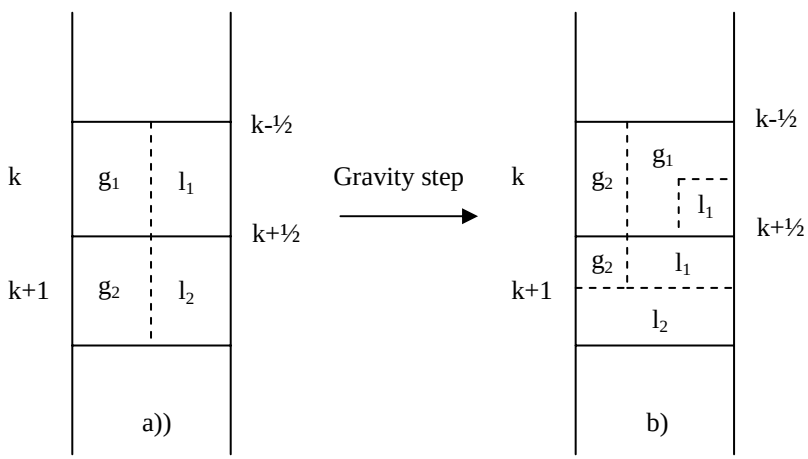

Figure 2: Pseudo-immiscible gravity segregation.

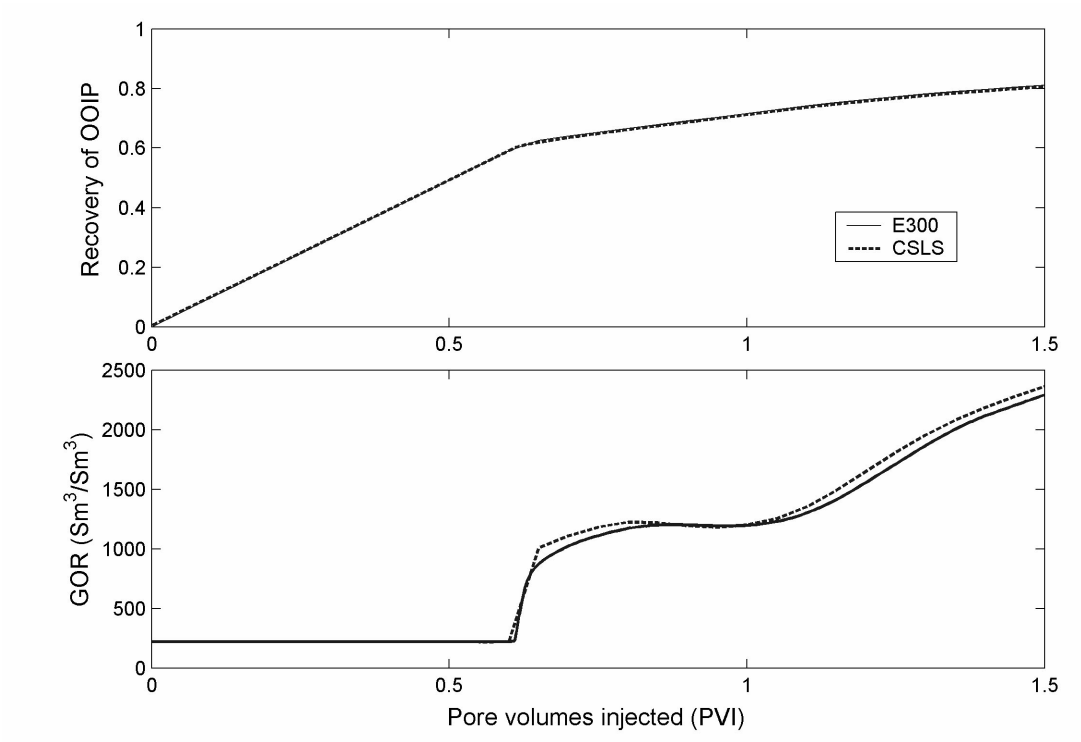

Figure 3: 1D displacement. Recovery and gas-oil ratio predicted by CSLS and E300

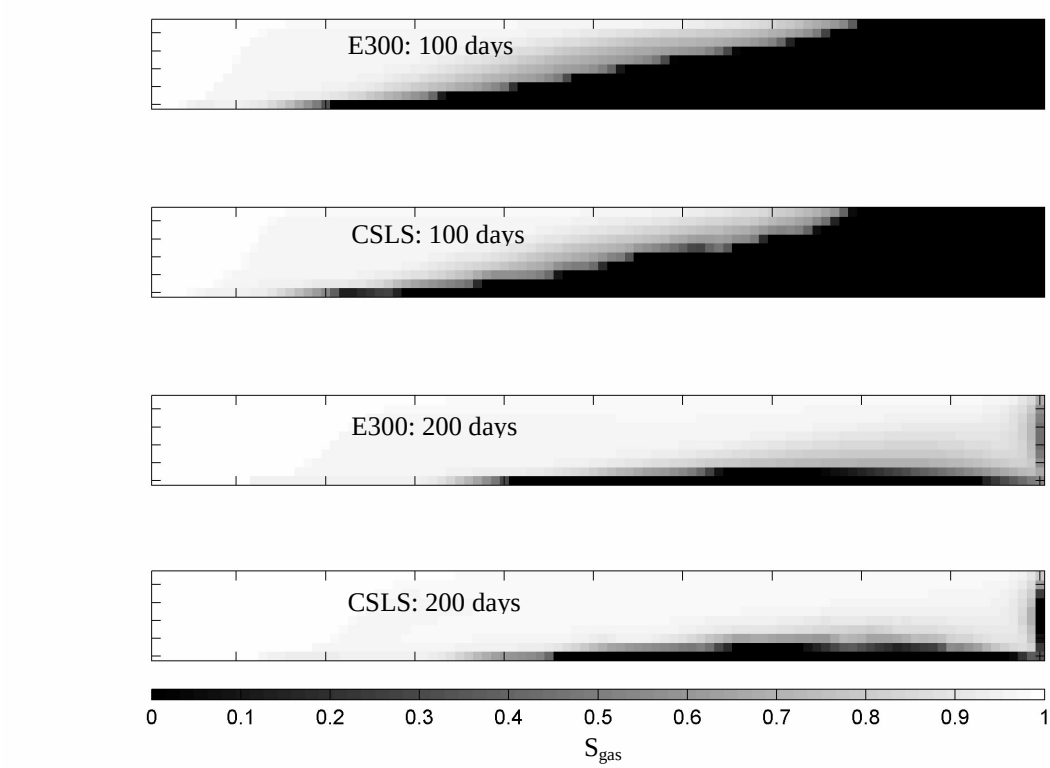

Figure 4: Comparison of gas saturation distribution for 2D homogeneous and anisotropic displacements (100 days = 0.5 PVI and 200 days = 1.0 PVI)

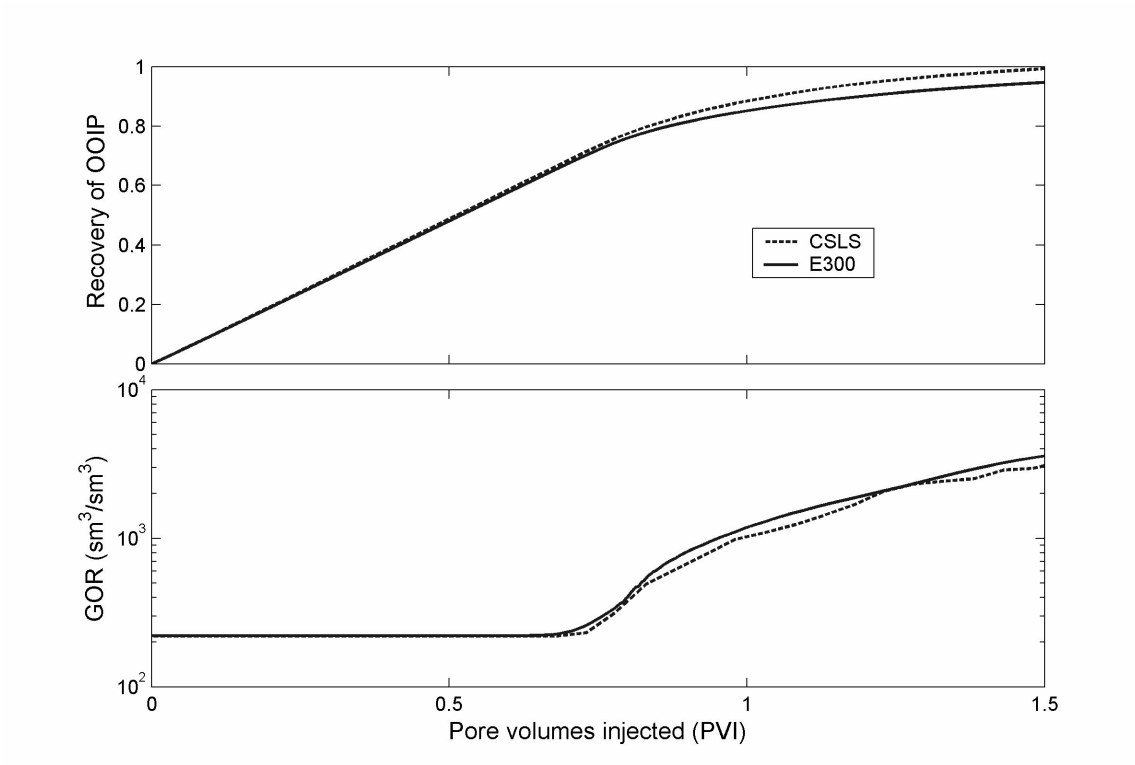

Figure 5: Oil recovery and gas-oil ratio for homogeneous displacement (E300 and CSLS)

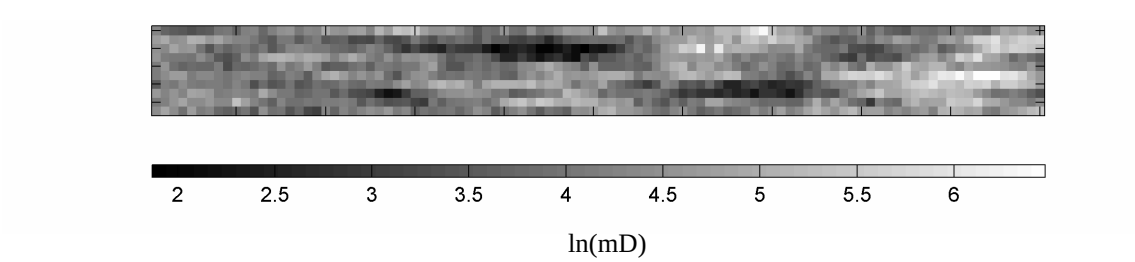

Figure 6: Permeability field, ln(K), for 2D displacement.

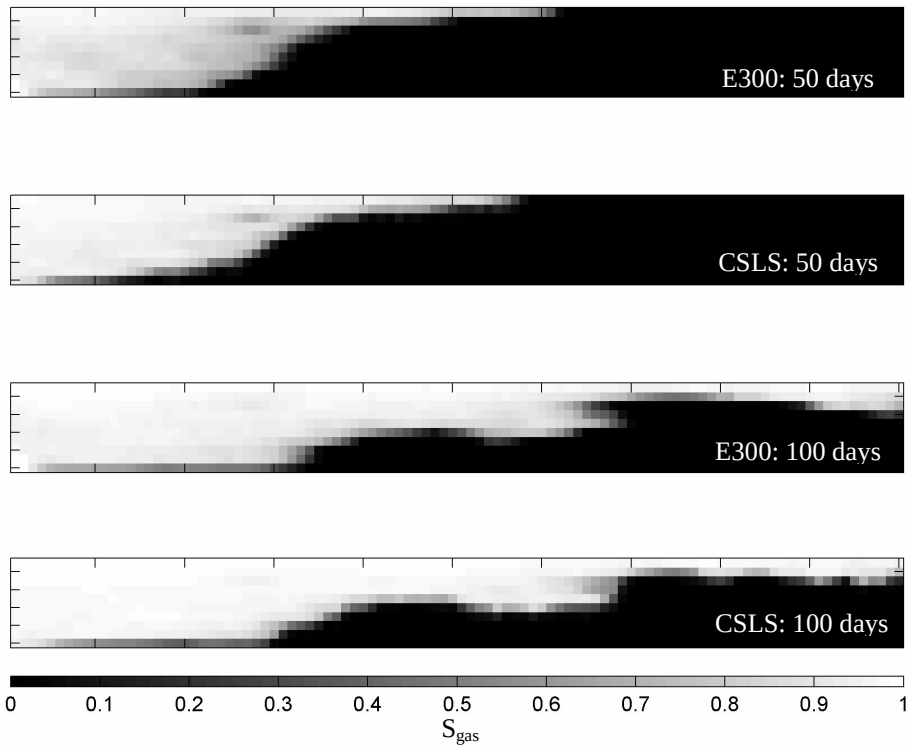

Figure 7: Gas saturation for 2D heterogeneous displacements (0.25 PVI and 0.5 PVI)

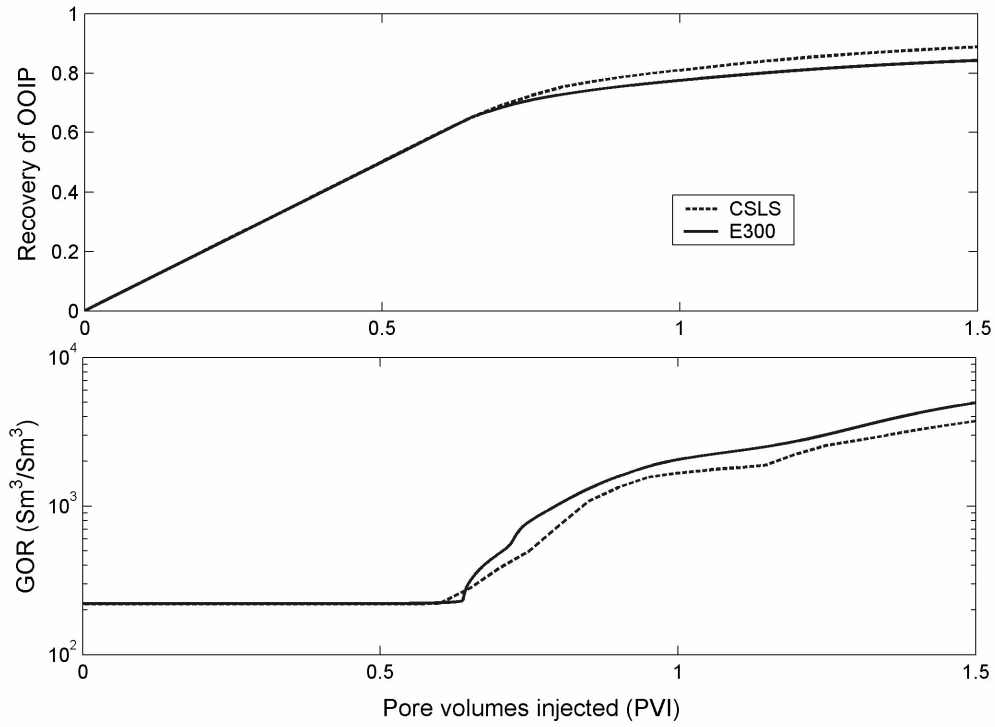

Figure 8: Comparison of recovery and gas-oil ratio for heterogeneous 2D displacement.

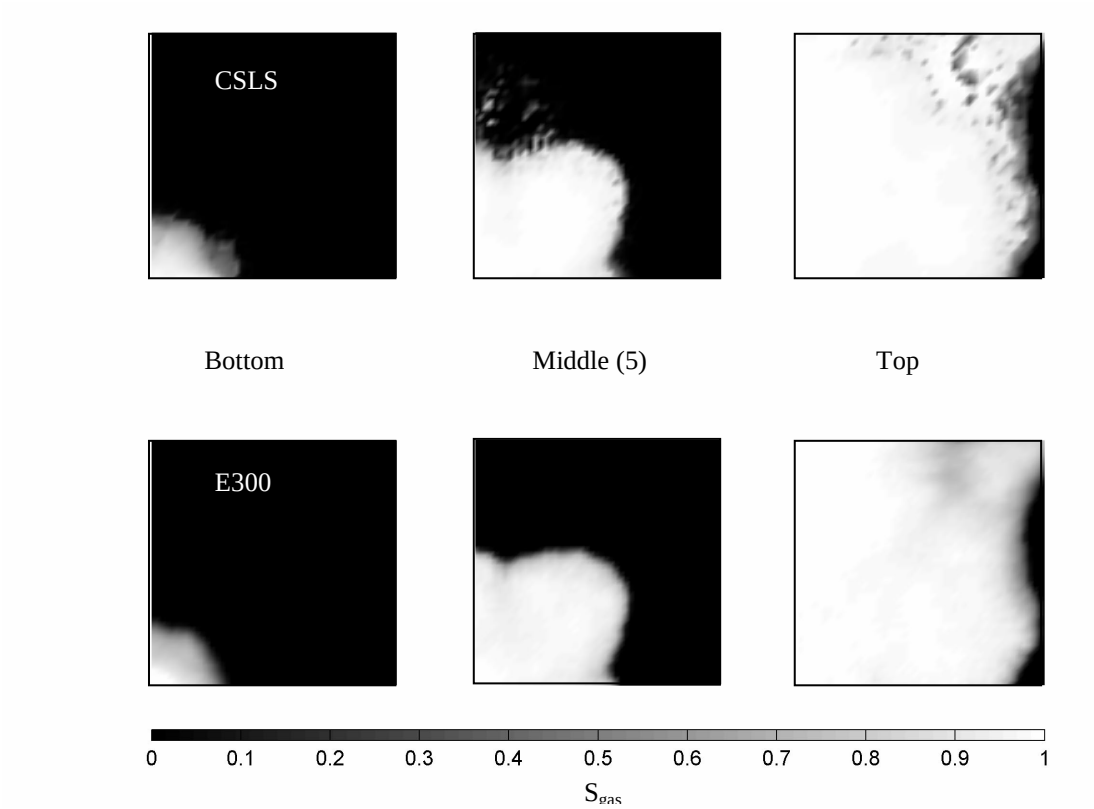

Figure 9: Gas saturation distribution for 3D heterogeneous quarter five-spot (0.3 PVI)

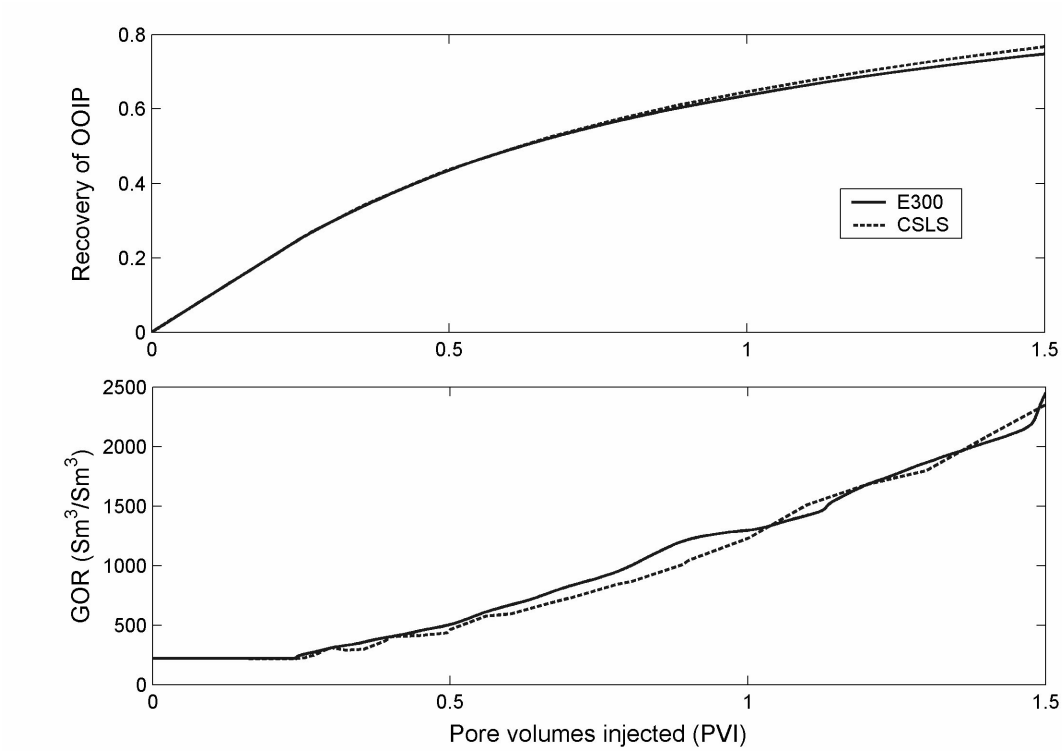

Figure 10: Comparison of recovery and gas-oil ratio for for 3D heterogeneous quarter five-spot.

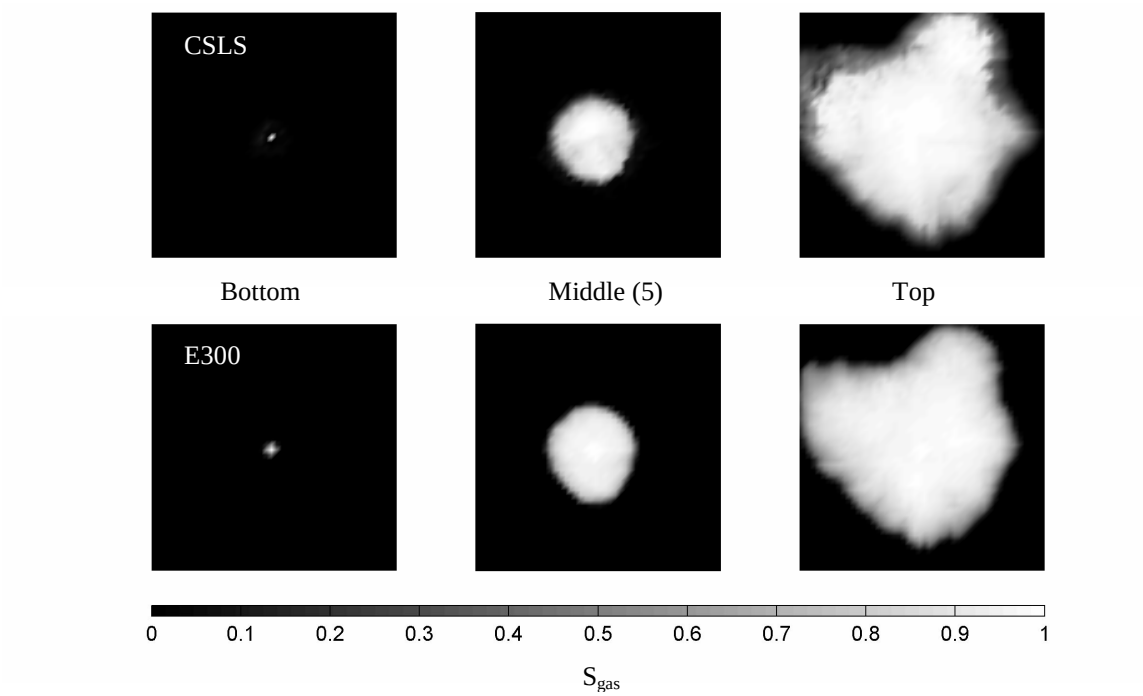

Figure 11: Gas saturation after 100 days of injection (0.1 PVI)

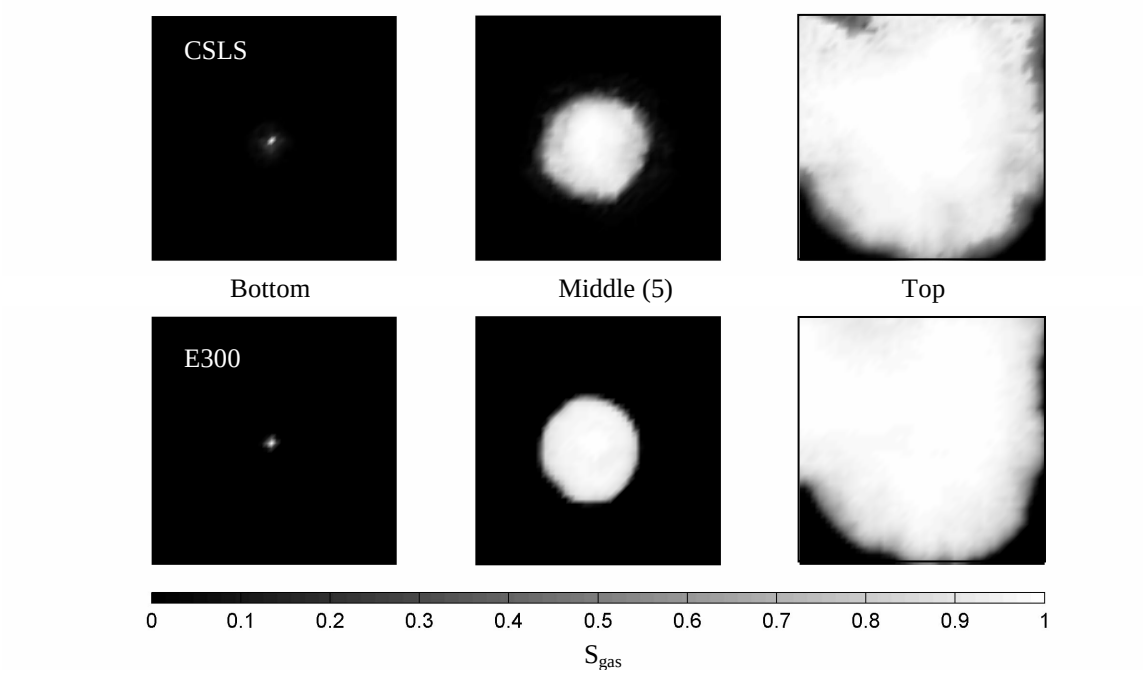

Figure 12: Gas saturation after 200 days of injection (0.2 PVI)

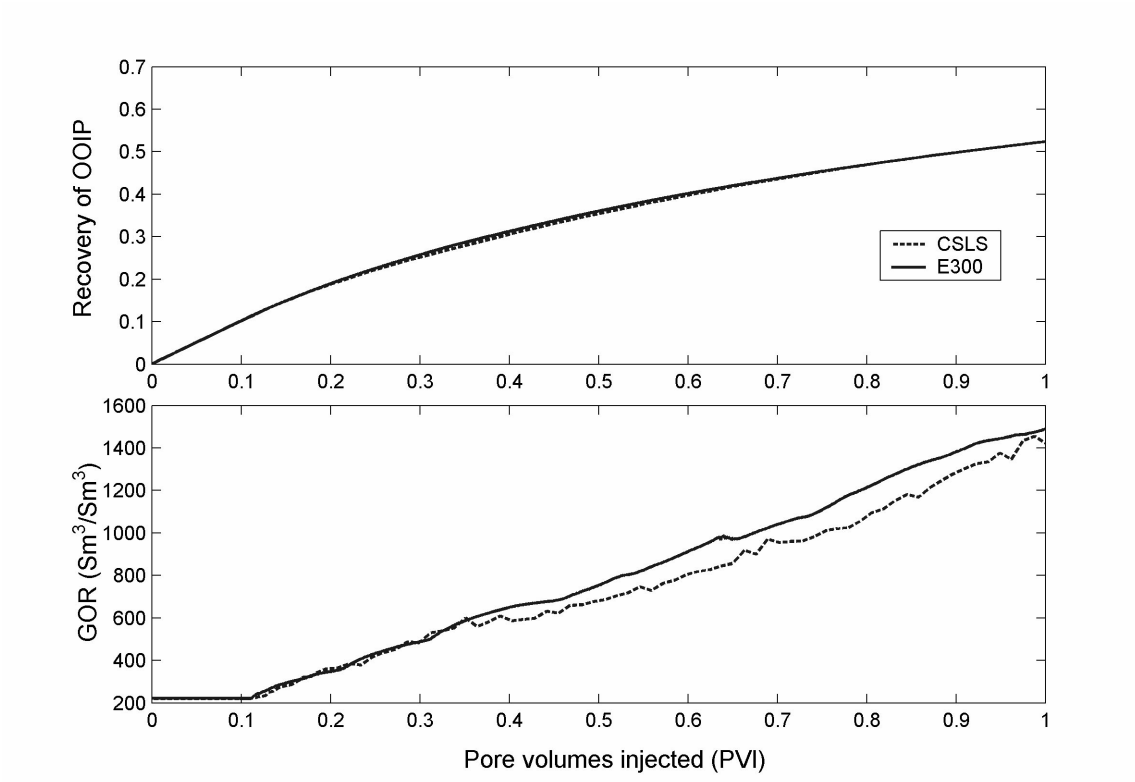

Figure 13: Comparison of oil recovery and gas-oil ratio for five-spot simulation.